Chaos in a System with a Periodically Disappearing Separatrix

VINCENT T. COPPOLA[1] and RICHARD H. RAND[2]

[1]*Concept Development Branch, Naval Research Laboratory, Washington, D.C. 20375. U.S.A.*
[2]*Department of Theoretical and Applied Mechanics, Cornell University, Ithaca, NY 14853, U.S.A.*

Abstract. We investigate the system $\ddot{x} - x\cos\varepsilon t + x^3 = 0$ in which $\varepsilon \ll 1$ by using averaging and elliptic functions. It is shown that this system is applicable to the dynamics of the familiar rotating-plane pendulum. The slow forcing permits us to envision an 'instantaneous phase portrait' in the $x - \dot{x}$ phase plane which exhibits a center at the origin when $\cos\varepsilon t \leq 0$ and a saddle and associated double homoclinic loop separatrix when $\cos\varepsilon t > 0$. The chaos in this problem is related to the question of on which side (left (= L) or right (= R)) of the reappearing double homoclinic loop separatrix a motion finds itself. We show that the sequence of L's and R's exhibits sensitive dependence on initial conditions by using a simplified model which assumes that motions cross the instantaneous separatrix instantaneously. We also present an improved model which 'patches' a separatrix boundary layer onto the averaging model. The predictions of both models are compared with the results of numerical integration.

Key words: Chaos, perturbation methods, elliptic functions, differential equations.

Introduction

This work concerns the dynamics of a slowly varying Hamiltonian system for which the 'instantaneous phase portrait' (i.e. the phase portrait for a fixed value of the forcing function) changes qualitatively with time. In particular we consider the following example suggested by Professor Philip Holmes of Cornell University:

$$\ddot{x} - x\cos\tau + x^3 = 0\,, \quad \tau = \varepsilon t, \quad \varepsilon \ll 1\,, \tag{1}$$

where $\dot{}$ represents differentiation with respect to time t. For τ fixed, the phase space is filled with closed orbits given by the Hamiltonian

$$\tfrac{1}{2}\dot{x}^2 - \tfrac{1}{2}x^2\cos\tau + \tfrac{1}{4}x^4 = h \tag{2}$$

where the energy h is not constant in time.

The sign of $\cos\tau$ determines the qualitative nature of the instantaneous phase portrait which contains either a center at the origin or a double homoclinic loop with saddle at the origin and centers to the left and right, see Figure 1. For $\cos\tau < 0$, all orbits are closed and encircle the center at the origin. For $\cos\tau > 0$, there are three regions of closed orbits separated by a double homoclinic loop which we shall refer to as an 'instantaneous separatrix'. Each loop encloses a center at $(\pm\sqrt{\cos(\tau)},\ 0)$, around which lies a family of closed orbits. A third family of closed orbits encircles the instantaneous separatrix. As τ changes, the instantaneous phase portrait changes so that the double homoclinic loop is born, grows to a maximum, shrinks back into the origin, lies dormant, and then is born again. This occurs smoothly and periodically.

We expect the system to be chaotic since after each birth of the double homoclinic loop, some

Nonlinear Dynamics **1**: 401–420, 1990

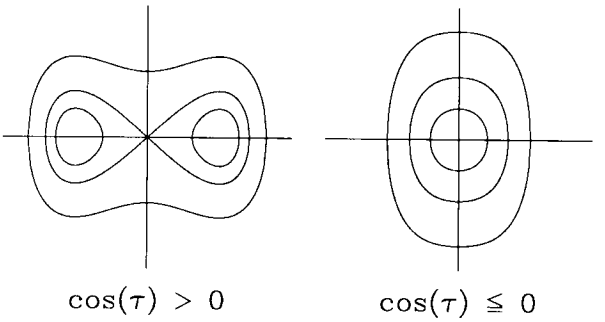

Fig. 1. The qualitative nature of the instantaneous phase portrait depends on the value of $\cos(\tau)$. For $\cos(\tau) > 0$, a separatrix divides the phase space into three regions; for $\cos(\tau) \leq 0$, no separatrix is present and all orbits encircle the origin.

trajectories will encircle the left (=L) center while others will encircle the right (= R) center. The sequence of L's and R's for a given trajectory will be shown to exhibit sensitive dependence on initial conditions.

As an example of the chaotic dynamics which occur in such a system, we consider the familiar rotating-plane pendulum [1, 12], Figure 2. A plane pendulum is forced to rotate about a vertical axis with angular velocity $\omega(t)$. The Lagrangian is

$$L = \frac{m}{2}\left[l\dot{\varphi}^2 + l^2\omega(t)^2 \sin^2\varphi\right] + m\,g\,l\cos\varphi \tag{3}$$

where m is the mass of the pendulum, l is its length and g is the acceleration of gravity. The corresponding equation of motion is

$$\ddot{\varphi} + \left[\frac{g}{l} - \omega(t)^2\cos\varphi\right]\sin\varphi = 0\,. \tag{4}$$

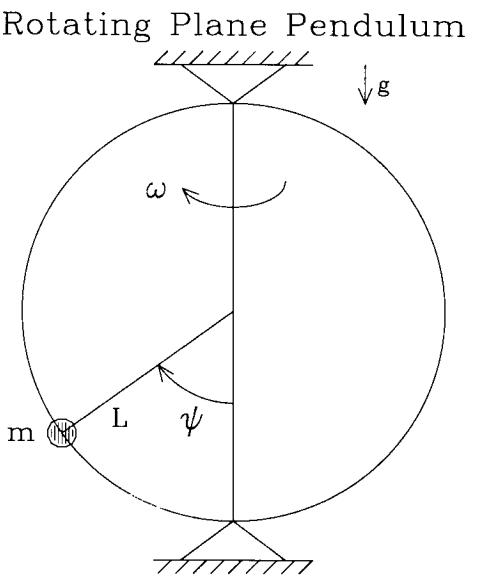

Fig. 2. The mass m slides (without friction) along a circular hoop of radius L making an angle of ψ with respect to the vertical. The hoop rotates along the vertical axis with angular velocity ω.

As is well known [1, 12], this system, for fixed ω, possesses 1 or 3 equilibria depending respectively on whether ω^2 is smaller or larger than g/l. In order to see the relation between equation (4) and equation (1), we use the following scalings:

$$\omega^2 = \frac{g}{l} + \varepsilon \cos(\varepsilon^{3/2} t), \quad \varphi = \varepsilon^{1/2} x, \quad t = \varepsilon^{-1/2} \eta. \tag{5}$$

Substituting equations (5) into equation (4) and expanding for small ε, we obtain

$$\frac{d^2 x}{d\eta^2} - x \cos(\varepsilon \eta) + \frac{g}{2l} x^3 + \cdots = 0 \tag{6}$$

where $\cdots$ represents terms of order ε. Note that (6) is of the form (1) for $g/l = 2$. In Figure 3 we present the results of numerical integration of equation (4) with ω defined as in (5), for $g/l = 2$ and $\varepsilon = 0.1$. Note how the numerically integrated trajectory changes from left to right separatrix loop in an unpredictable fashion.

In this paper, we apply the method of averaging to equation (1) using elliptic functions. We

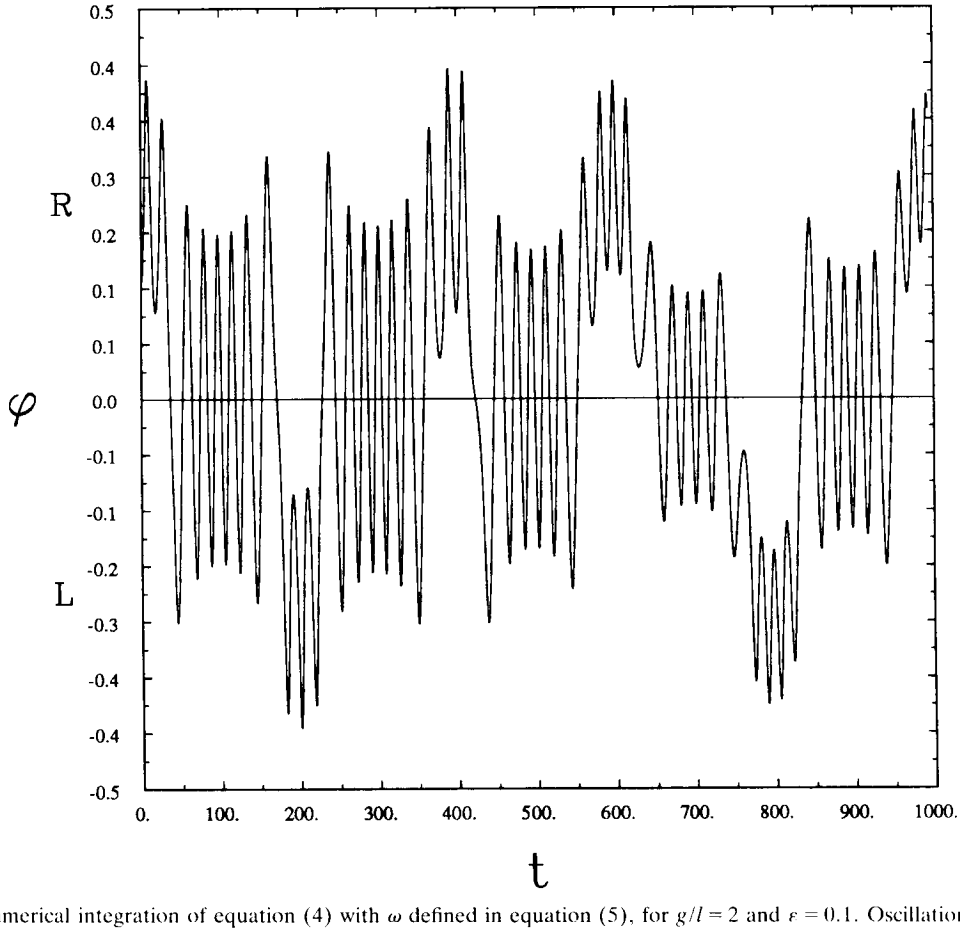

Fig. 3. Numerical integration of equation (4) with ω defined in equation (5), for $g/l = 2$ and $\varepsilon = 0.1$. Oscillations about a positive value of φ are located within the right instantaneous separatrix loop; those about a negative value are located within the left loop. Oscillations about $\varphi = 0$ are located outside the separatrix (if it exists at that time) or the origin.

first present a simplified model based on the averaged system which assumes that motions cross the instantaneous separatrix instantaneously. We show that this model is chaotic (without the aid of the Melnikov function [13, 22], which cannot be applied here since the separatrix periodically disappears.) We also present an improved model which 'patches' a separatrix boundary layer onto the averaging model. The behavior of both models is compared with numerical integrations of equation (1).

Finally, we give a word of caution. For τ varying, equation (1) is a forced one degree of freedom problem with phase space $\mathbb{R}^2 \times S^1$. But since τ varies slowly and we know the solution at every fixed τ, we choose to view the problem by projecting onto $\mathbb{R}^2$. In this way, we view equation (1) as a system with a slowly oscillating instantaneous phase protrait. We wish to make clear, however, that the instantaneous phase portraits are not really part of the dynamics; they only aid in our understanding and analysis. Hence, when we speak of the separatrix it is clear that we mean the separatrix in the instantaneous phase portrait and *not* in the real system itself. Likewise, instantaneous centers inside each loop of the separatrix are not fixed points in the real system. Equation (1) admits only one fixed point, the origin.

Averaging

In order to apply the method of averaging [21] to equation (1), we first obtain a general solution to (1) with τ treated as a constant ('the unperturbed equation'). This general solution will contain two arbitrary constants and will involve elliptic functions. Then we use variation of parameters to obtain differential equations on the arbitrary constants such that (1) is satisfied when $\tau = \varepsilon t$. Finally we average the latter differential equations over the period of the unperturbed equation, assuming $\varepsilon \ll 1$. See [7] for a similar treatment of a related problem.

In Appendix I we show that the general solution to equation (1) for all *fixed* τ can be written in the form:

$$x = \mu\, r\, \mathrm{cn}(u, k)\,, \quad \dot{x} = \mu\, r\, a\, \mathrm{cn}'(u, k) \tag{7}$$

where $\mathrm{cn}(u, k)$ is a Jacobi elliptic function with argument u and modulus k, and where $'$ represents differentiation with respect to the argument u. In the rest of the paper we will abbreviate $\mathrm{cn}(u, k)$ by simply writing cn, and similarly for the elliptic functions sn and dn. The argument u and modulus k are given by:

$$u = a\, t + b\,, \quad k^2 = \frac{r^2}{2a^2} \tag{8}$$

where

$$a^2 = r^2 - \cos\tau$$

and where r and b are arbitrary constants. All of the possible cases of trajectories lying both inside and outside of the instantaneous separatrix (see Appendix I) are included in the following parameter ranges:

$$a \geq 0\,, \quad \infty \geq b > 0\,, \quad r^2 \geq \cos\tau\,, \quad r \geq 0\,, \quad \mu = \pm 1$$

where r and b are independent constants. As shown in Appendix I, the cn function is strictly positive for motions which lie inside the instantaneous separatrix loops. The parameter μ is used to distinguish motions lying in the left loop from those in the right loop.

We are now ready to apply the method of variation of parameters. Instead of r and b we choose

$$\rho = r^2 \tag{9}$$

and u as our parameters to be varied. The details are given in Appendix II, with the resulting equations:

$$\dot{\rho} = -2\varepsilon k^2 \,\mathrm{sn}^2 \sin\tau \tag{10}$$

$$\dot{u} = a + \varepsilon \frac{1}{\rho}\left(\frac{1}{\mathrm{dn}}\,\mathrm{dn}' - 2k^3 \frac{\mathrm{d}u}{\mathrm{d}k}(2\,\mathrm{dn}^2 - \mathrm{cn}^2)\right)\sin\tau\,. \tag{11}$$

We wish to apply the method of averaging to equations (10), (11). Although the $\dot{\rho}$ equation is periodic in u (the functions cn, sn, and dn are all periodic in u with periods $4K(k)$, $4K(k)$, and $2K(k)$ respectively), the $\dot{u}$ equation is not (because of the $\mathrm{d}u/\mathrm{d}k$ term which grows linearly in u, see Appendix II). This arises from 'phase shear' in the τ-fixed systems, i.e., the dependence of frequency on amplitude, giving rise to an unbounded growth in phase differences between neighboring orbits. We may however replace u by a new variable φ which is defined so as to take account of the dependence of frequency on amplitude, and which results in the $\dot{\varphi}$ equation being periodic in φ (see Appendix II):

$$\varphi = \frac{u}{4K} \text{ where } K = K(k) \tag{12}$$

$$\dot{\varphi} = \frac{a}{4K} - \frac{\varepsilon \sin\tau}{4K(\rho - \cos\tau)(\rho - 2\cos\tau)} \times [\mathrm{cn}\,\mathrm{cn}'\cos\tau + Z(u)(\rho - 2\cos\tau + \mathrm{cn}^2\cos\tau)] \tag{13}$$

where $Z(u) = E(u) - (E/K)u$ is an odd $2K(k)$ periodic function called the Jacobi zeta function [3]. Here $E(u)$, E $(= E(k))$ and K $(= K(k))$ are respectively the incomplete elliptic integral of the second kind, the complete elliptic integral of the second kind, and the complete elliptic integral of the first kind.

In fact, φ is the angle variable associated with the action-angle variables [11] of equation (1). The action variable J for equation (1) with τ fixed is defined as the area enclosed by an orbit:

$$J = \oint \dot{x}\,\mathrm{d}x$$

which may be evaluated using equation (7) as:

$$J = \frac{4\rho}{3k^2}\, a[(2k^2 - 1)E + (1 - k^2)K]\,. \tag{14}$$

Our choice of ρ rather than J as our amplitude-like variable is due to the fact that equation (14) cannot be solved for h in explicit form (because E and K depend on k which depends on h). In the case of ρ, we find by substituting (7) into (2):

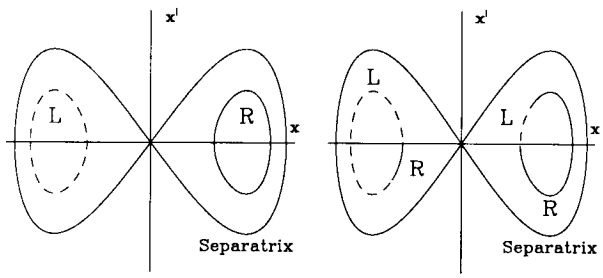

Fig. 4. The Poincaré map P defined by the averaged equations is displayed above. The curves L (indicating Left) and R (indicating Right) are mapped by P onto themselves with an interval exchange and a rotation. In this way, points originally on the right can be mapped onto the left and vice versa.

$$h = \tfrac{1}{4}\,\rho(\rho - 2\cos\tau)\,. \tag{15}$$

We are now ready to average equations (10), (13) assuming $\varepsilon \ll 1$. Holding ρ and τ fixed, we replace the right hand sides of (10), (13) by

$$\frac{1}{4K}\int_0^{4K} \cdots \mathrm{d}u$$

yielding the averaged equations:

$$\dot{\rho} = -2\varepsilon\left(1 - \frac{E}{K}\right)\sin\tau \quad \text{or} \quad \frac{\mathrm{d}\rho}{\mathrm{d}\tau} = -2\left(1 - \frac{E}{K}\right)\sin\tau \tag{16}$$

$$\dot{\varphi} = \frac{a}{4K}\,. \tag{17}$$

From (8), (9) and (16) we find an averaged equation on the auxiliary quantity

$$m = k^2 \tag{18}$$

$$\frac{\mathrm{d}m}{\mathrm{d}\tau} = (1 - 2m)\left[m - (2m - 1)\left(1 - \frac{E}{K}\right)\right]\tan\tau\,. \tag{19}$$

Equation (19), in contrast to equation (16), is separable, since E and K depend only on m. However, (19) is not integrable in closed form. Thus we prefer to work with (16), since the amplitude variable ρ is easier to interpret physically than the modulus variable m.

Analysis of the Averaged Equations

Equation (16) is defined on the half-cylinder $\mathscr{H} = \{(\rho, \tau)\varepsilon\mathbb{R}^+ \times S\}$. Since both E and K depend on the modulus k, which, from (8), (9) may be written

$$k = \left(\frac{\rho}{2(\rho - \cos\tau)}\right)^{1/2} \tag{20}$$

we see that the slope field of (16) is an odd function of τ on $\mathscr{H}$. Thus the transformation $\tau \to -\tau$ leaves (16) invariant, and all orbits are symmetric about the line $\tau = 0$. Since (16) has no singularities, there can be no equilibria in the flow on $\mathscr{H}$. Moreover no orbits can escape to infinity since for large ρ, $k \sim 1/\sqrt{2}$, $E \sim 1.350644\ldots$, $K \sim 1.854075\ldots$, so that (16) gives $d\rho/d\tau \sim -0.543053\ldots \sin\tau$ and $\rho \sim 0.543053\ldots \cos\tau + \rho_0$, which is a closed orbit. The possibility of limit cycles in the flow on $\mathscr{H}$ is precluded by the Hamiltonian nature of the unperturbed problem. Thus all orbits are closed and we may conclude that for arbitrary initial conditions, $\rho(\tau)$ is an even 2π-periodic function.

This result is illustrated in Figure 5, which shows the results of numerical integration of equation (16). As ρ changes, a given motion moves (slowly, since τ is slow time) from one instantaneous energy curve (2) to another. In order to display the instantaneous position of the separatrix, we note from (2) that since it passes through the origin $x = \dot{x} = 0$, the separatrix corresponds to $h = 0$. Then from (15) we find

$$\text{separatrix: } \rho = 2\cos\tau > 0\,. \tag{21}$$

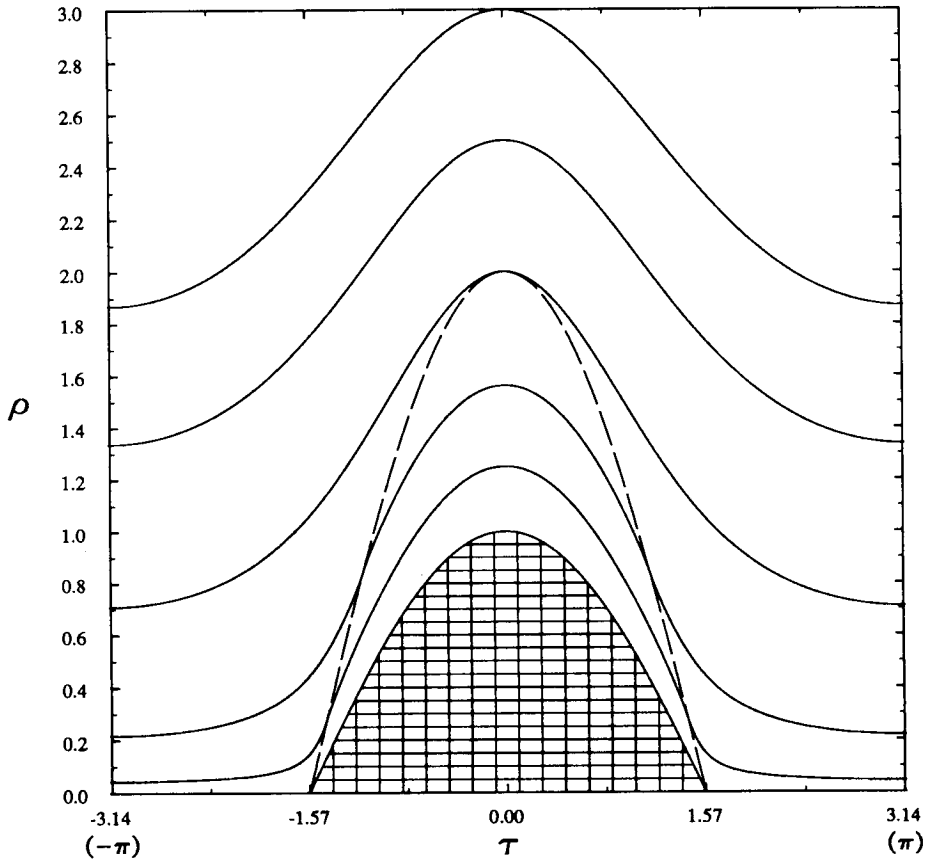

Fig. 5. Numerical integration of equation (16) on the (ρ, τ) cylindrical phase space. The separatrix condition (equation (21)) is shown dashed; some orbits cross this curve (corresponding to crossing into or out of a separatrix loop) while others do not. We denote by τ_s the time τ at which an orbit starting at $\tau = 0$ first crosses the separatrix condition curve (for orbits which do cross). The gridded region is unmeaningful for the model and should be ignored.

As expected, we see from Figure 5 that some motions always remain outside the separatrix ($h > 0$), while others cross through it, moving between inside the separatrix ($h < 0$) and outside the separatrix. We shall assume for the present that motions which cross the instantaneous separatrix, do so instantaneously. This assumption furnishes us with a simplifed model which may be easily analyzed. Later in this paper we shall examine the shortcomings of this assumption, and we shall replace this simplified model with an improved model.

Note in Figure 5 that the region of $\mathcal{H}$ lying between $\rho = 0$ (the origin) and $\rho = \cos\tau$ (the instantaneous centers lying inside the homoclinic loops) is unreachable from any physically meaningful initial conditions and should be ignored.

Next let us consider equation (17) on $d\varphi/dt$. From the fact that $\rho(\tau)$ is an even 2π-periodic function, it follows that so are $r(\tau)$, $a(\tau)$ and $k(\tau)$. This makes $d\varphi/dt$ an even 2π-periodic function of τ with a nonzero mean. Hence $\varphi(\tau)$ can be written as:

$$\varphi(\tau) = \varphi_{av}\tau + \varphi_{per}(\tau) + \varphi_0 \tag{22}$$

where $\varphi_{per}(\tau)$ is an odd 2π-periodic function. Both φ_{av} and $\varphi_{per}(\tau)$ depend on ρ_0, the initial value of ρ, but are independent of φ_0.

In order to better understand the dynamics of the averaged system, we consider a Poincaré map P. We choose the surface of section

$$\Sigma: \{(x, y, \tau) | \tau = 0 (\mathrm{mod}\, 2\pi)\} \tag{23}$$

where the values of x and $y = \dot{x}$ are given by equations (7). Alternately we may view P as mapping $(\rho, \varphi)_{\tau=0}$ to $(\rho, \varphi)_{\tau=2\pi}$, which results in, from the fact that $\rho(\tau)$ is 2π-periodic and from equation (22):

$$P: (\rho_0, \varphi_0) \rightarrow (\rho_0, 2\pi\varphi_{av} + \varphi_0)\,. \tag{24}$$

Since ρ is unchanged in (24), we see that instantaneous energy curves at $\tau = 0$ remain invariant under the Poincaré map P. For those curves which lie outside the separatrix at $\tau = 0$ (corresponding to $h > 0$ in equation (15)), equation (24) shows that P simply represents a rotation resulting from a change of $2\pi\,\varphi_{av}$ in φ.

However, the situation for those instantaneous energy curves which lie inside of the double loop separatrix at $\tau = 0$ is more interesting. For given ρ_0 (and hence given $h < 0$ in equation (15)), there are two such disconnected closed curves (L = left, R = right), each lying within its own homoclinic loop. The Poincaré map P maps the set of points {L, R} onto itself.

Let τ_s be the slow time between $\tau = 0$ and the crossing of the separatrix. From Figure 5, $\tau_s < \pi/2$. Since τ_s is determined by equation (16) on ρ without use of equation (17) on φ, it is clear that τ_s depends on ρ_0 but not on φ_0, i.e., all points on a given instantaneous energy curve reach the separatrix at the same instant. Then the motion generating P may be decomposed into three stages:

1: $0 < \tau < \tau_s$, during which time a motion remains inside its original homoclinic loop,
2: $\tau_s < \tau < 2\pi - \tau_s$, during which time the motion lies outside of the separatrix, and
3: $2\pi - \tau_s < \tau < 2\pi$, during which time the motion lies inside one of the homoclinic loops, *but possibly not the loop within which the motion started.*

Let us consider the changes occurring during each of these stages. We will follow a typical set of points, call them C, which are located on instantaneous energy curves L and R at $\tau = 0$. At the end of stage 1 the points C have moved to new instantaneous energy curves lying just inside of the left and right homoclinic loops respectively. During stage 1, the separatrix loops have themselves changed shape, becoming smaller with increasing τ. See Figure 6. We denote by φ_s the change in φ accompanying this motion, and find from (22),

$$\Delta\varphi \text{ for stage 1: } \varphi_s = \varphi_{\text{av}}\tau_s + \varphi_{\text{per}}(\tau_s)\,. \tag{25}$$

During stage 2, all of the points in C find themselves on the same instantaneous energy curve, located outside of the separatrix, see Figure 6. Stage 2 lasts more than half of the forcing period, during which time the separatrix shrinks to a point, disappears, and then reappears and grows to the same size it was at the beginning of stage 2. The change in φ during stage 2 is, from (22),

$$\Delta\varphi \text{ for stage 2: } \varphi(2\pi - \tau_s) - \varphi(\tau_s) = (2\pi - 2\tau_s)\varphi_{\text{av}} - 2\varphi_{\text{per}}(\tau_s) = 2\pi\varphi_{\text{av}} - 2\varphi_s \tag{26}$$

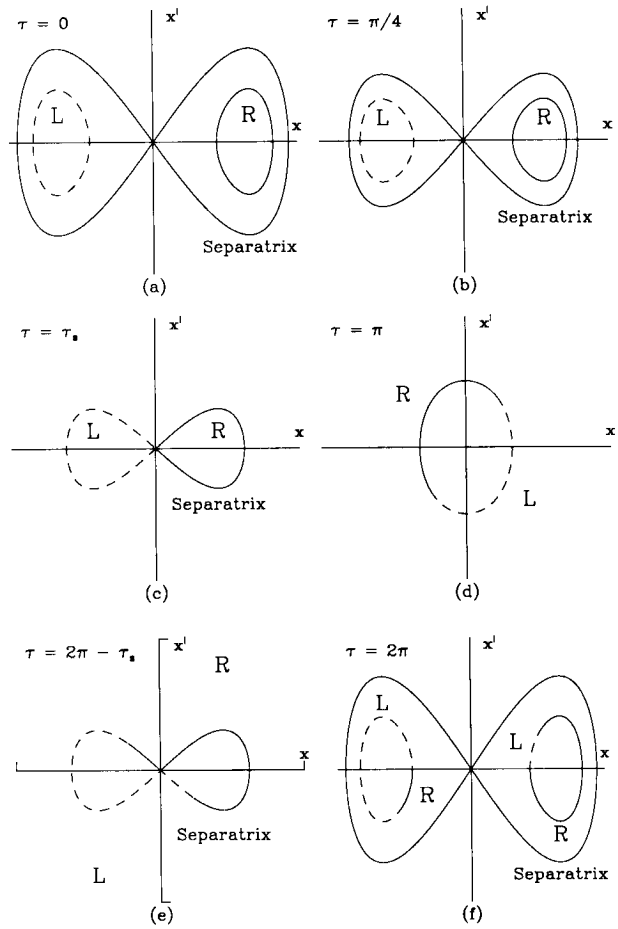

Fig. 6. The six pictures (a–f) show the motion of the two initial curves L and R displayed in (a) through one 2π period in τ. The motion can be divided into three stages, see the text. The Poincaré map is shown in (f).

where we have used the fact that $\varphi_{\text{per}}(\tau)$ is an odd 2π-periodic function. At the beginning of stage 3, the set C is once again located on two disconnected instantaneous energy curves which are just inside of the two separatrix loops. By symmetry, the change in φ accompanying stage 3 is the same as that for the stage 1:

$$\Delta\varphi \text{ for stage 3: } \varphi_s = \varphi_{\text{av}}\tau_s + \varphi_{\text{per}}(\tau_s)\,. \tag{27}$$

At the end of stage 3, the set C has returned to its original position. However, because of the phase flow φ during stage 2, some points which were originally on curve L are now on curve R and vice versa.

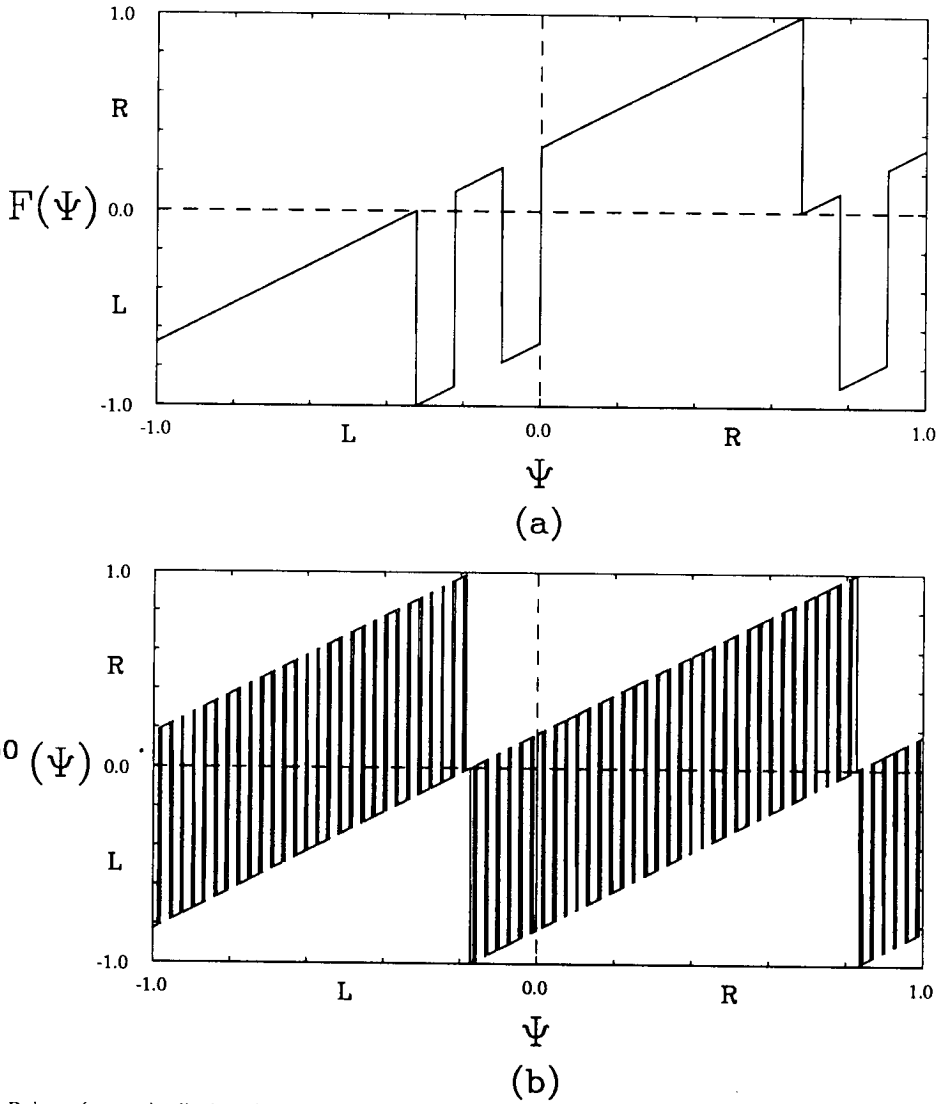

Fig. 7. The Poincaré map is displayed as the interval exchange map $F(\psi)$ in (a). Each point on C (where $C = \text{L} \cup \text{R}$) corresponds to a unique ψ value which gets mapped under F to another point of C. F is composed of an exchange of an interval between R and L and a translation in ψ. The 50th iterate of F, which shows many exchanged intervals, is shown in (b).

The effect of the Poincaré map P on the set $C = \{L, R\}$ may thus be described as a rotation of magnitude (from (25), (26) and (27)):

$$2\pi\varphi_{av} \tag{28}$$

combined with an interchange of two intervals between L and R. The magnitude of the interchanged intervals is, from (26),

$$2\pi\varphi_{av} - 2\varphi_s \,. \tag{29}$$

The endpoints Q of the interchanged intervals separate initial conditions which end up on opposite sides of the homoclinic loops after one forcing period.

The Poincaré map P may be characterized by a one dimensional discontinuous function $F(\psi)$ which maps the set C onto itself. ($F(\psi)$ is an example of an *interval exchange map* [16].) If we parameterize C by letting ψ go from -1 to 0 on L and from 0 to 1 on R, then the graph of the function $F(\psi)$ lies in the square region $[-1, 1) \times [-1, 1)$ and is displayed in Figure 7a.

As we vary the particular instantaneous energy curve C on which P so acts, the magnitude of the rotation, $2\pi\varphi_{av}$, varies continuously. In general this magnitude will be incommensurate with the circumference of the instantaneous energy curve C, which is 2 when measured in ψ, and so we are generically dealing with an irrational flow on S^1 [1]. If the mapping P is iterated, the set of endpoints Q will continue to grow, and in the limit as $\tau \to \infty$, this set will be dense in C. Thus the sequences of L's and R's corresponding to a particular point on C will be different from those of other neighboring points on C. This implies sensitive dependence on initial conditions, a criterion often used to describe chaos [9]. In terms of the Poincaré map function $F(\psi)$ shown in Figure 7a, high iterates of $F(\psi)$ will contain many points of discontinuity, see Figure 7b.

For a set of instantaneous energy curves of measure zero, however, the rotation magnitude will be commensurate with the circumference of the instantaneous energy curve C and the action of P will be that of a rational flow on S^1. In this nongeneric case no chaos will result, as the model predicts periodic orbits.

Comparison of the Simplified Model with the Original System

The foregoing analysis of chaos in equation (1) is approximate. In order to test the validity of the approximation, we compare the predictions of the averaged equations with the results of numerical integration of equation (1).

In order to generate a numerical version of the Poincaré map P, cf. equations (23), (24), we choose an initial condition $(x(0), \dot{x}(0))$ and integrate equation (1) from $t = 0$ to $t = 2\pi/\varepsilon$. For a comparison with the averaging results, we choose a number of initial conditions all lying on the same instantaneous energy curve corresponding to a given value of the energy h. Figure 8 shows the result for $\varepsilon = 0.1$.

Many of the mapped points lie in a neighborhood of the right (= R) or left (= L) instantaneous energy curves corresponding to the energy h, as predicted by the averaging analysis. However, some points lie on 'threads' which reach from one side of Figure 6 to the other, winding around R and L, and lying close to the 'instantaneous unstable manifold' associated with the instantaneous separatrix of equation (2) for $\tau = 0$. The threads are created as motions approach

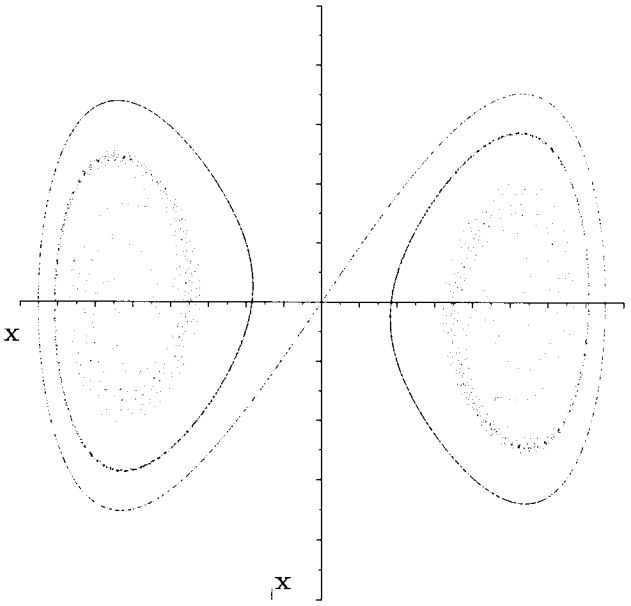

Fig. 8. The Poincaré map of equation (1), computed using numerical integration, for the same initial conditions (L and R) as shown in Figure 4.

the instantaneous unstable manifold and get stretched apart. The threads represent a continuous version of the jump which was predicted at the ends of the interchanged intervals, cf. Figure 6. However, the nature of the intervals which are interchanged is much more complicated in the numerical integration results than in the averaging results. Instead of just a single interval being interchanged, as in Figure 6, we find that many intervals are interchanged.

Examination of the Poincaré maps shown in Figure 6 and Figure 8 shows that the simplified model is unable to portray the dynamics of equation (1) in the neighborhood of the threads. A more careful analysis of the numerical integration that created Figure 8 shows that *while the threads make up a large portion of the picture, they arise from very tiny intervals of the original initial energy curves L and R* (some intervals as small as 10^{-10} in length).

Thus, while the simplified model offers an explanation of the chaos in equation (1) which is in qualitative agreement with the kind of unpredictable behavior seen numerically, cf. Figure 3, its results are not asymptotically valid, i.e., the difference between the behavior of the simplified model and the original system does not approach zero as $\varepsilon \to 0$.

A closer inspection of the averaging scheme reveals two technical problems which arise for $m = 1$ (the separatrix):

(i) φ in equation (12) is undefined at $m = 1$ (because $K = \infty$) so that equation (13) is meaningless, and

(ii) equation (16) is not differentiable, so that solutions to equation (16) are not unique.

From this point of view the separatrix is a singular region at which the transformation to (ρ, φ) coordinates is ill-defined. Once a motion reaches the instantaneous separatrix, its future motion is not uniquely specified, i.e., the location of where and when it gets off the separatrix is unknown. In our analyis so far we have assumed that such a motion gets off the separatrix at the same point at which it gets on, i.e., *crossing is instantaneous*. We will show that some of the

differences between the simplified model and the results of numerical integration of equation (1) are due to this assumption.

Various researchers have offered suggestions of how to deal with separatrix crossing in a more accurate fashion. Cary *et al.* [4] and Henrard [14] have both investigated in great detail changes in the adiabatic invariant J during separatrix crossing in a Hamiltonian system. Cary and Skodje [5] extended [4] to include estimates for phase changes resulting from separatrix crossings. Escande [10], Menyuk [18] and Wiggins [25] have dealt with chaos in systems with slowly pulsating separatrices. Sanders and Verhulst [21], Kath [15] and Kevorkian and Cole [17] have addressed the separatrix crossing problem by using matched asymptotic expansions, viewing the region near the separatrix as a boundary layer. We will take this approach in creating an improved model of equation (1), i.e., we will augment the averaging model with a boundary layer model applicable in a neighborhood of the instantaneous separatrix.

An Improved Model: The Separatrix Boundary Layer

In this section, we will derive a separatrix crossing model based on the *unaveraged* equations (10), (11), valid in a boundary layer (abbreviated b.l. in what follows) around the separatrix. Since $m = 1$ corresponds to the separatrix at any time τ, we take (m, u) as variables, with the b.l. corresponding to values of m near unity (m is defined by equation (18)). Using equations (18), (8) and (9), we may rewrite equation (10) as an equation on m, whereupon equations (10), (11) on m and u become:

$$\dot{m} = \varepsilon m(1-2m)\tan\tau[1+(1-2m)\,\mathrm{sn}^2] \tag{30}$$

$$\dot{u} = a + \varepsilon\frac{1}{\rho}\left(\frac{1}{\mathrm{dn}}\,\mathrm{dn}' - 2k^3\frac{\mathrm{d}u}{\mathrm{d}k}(2\,\mathrm{dn}^2 - \mathrm{cn}^2)\right)\sin\tau\,. \tag{11}$$

We take $m = 1 + \varepsilon\sigma$, and expand equations (30), (11) in a Taylor series about $m = 1$:

$$\dot{\sigma} = -\tan\tau\,\mathrm{sech}^2(u) + O(\tan\tau[\varepsilon\,\sigma + \varepsilon^2\,\sigma^2\,e^{2u}]) \tag{31}$$

$$\dot{u} = \sqrt{\cos(\tau)} + O(\varepsilon\,\sigma + \tan\tau[\varepsilon + \varepsilon^2\,\sigma\,e^{2u}])\,. \tag{32}$$

We see from the order estimates that equations (31), (32) are valid for $|u| < u_{\max} < \infty$, i.e. away from the origin (where $u = \infty$). Under this condition, we use the truncated system to model the separatrix crossing:

$$\dot{\sigma} = -\tan\tau\,\mathrm{sech}^2(u) \tag{33}$$

$$\dot{u} = \sqrt{\cos(\tau)}\,. \tag{34}$$

In using equation (34), we have made an approximation for the $\dot{u}$ equation by assuming that the first term in equation (32) is the leading order term for any τ where $\cos(\tau) > 0$. This assumption is invalid only for values of τ near $\cos(\tau) = 0$. We propose to supplement the averaging model with a separatrix crossing condition based on the approximate equations (33), (34).

We now apply the two-variable expansion method in the timescales t and τ to equations (33) and (34). Letting $\sigma = \sigma(t, \tau)$ and $u = u(t, \tau)$, we find from (34)

$$u = \sqrt{\cos(\tau)}\,(t - t_*) + u_* \,. \tag{35}$$

Dividing (33) by (34) and integrating, we obtain

$$\sigma = -\frac{\tan\tau}{\sqrt{\cos(\tau)}}\,[\tanh(u) - \tanh(u_*)] + \sigma_* \tag{36}$$

where (σ_*, u_*, t_*) are the initial values of (σ, u, t) when the motion first reaches the b.l. The values (σ_*, u_*, t_*) will be obtained by patching the averaging model to equations (35), (36) at the b.l.

Although equations (35) and (36) offer an approximation for the separatrix crossing away from the origin, they are not valid near the origin (since the order estimates in equations (31), (32) are not valid there.) In order to model motions which cross the instantaneous separatrix near the origin, we proceed as follows. Scaling x by $x(t) = \delta\hat{x}(\tau)$, $\delta \ll 1$, and letting $\tau = \varepsilon\, t$, equation (1) becomes:

$$\varepsilon^2 \hat{x}_{\tau\tau} - \cosh(\tau)\,\hat{x} + \delta^2\,\hat{x}^3 = 0 \tag{37}$$

where subscript τ represents differentiation. To lowest order in δ we ignore the $\hat{x}^3$ term and apply the WKB method to find that to leading order in ε [2, 23]

$$\hat{x} = \hat{x}(\tau_*)\cos(l(\tau)/\varepsilon) + \varepsilon\,\frac{\hat{x}_\tau(\tau_*)}{\sqrt{\cos(\tau_*)}}\sinh(l(\tau)/\varepsilon) \tag{38}$$

$$\text{where } l(\tau) = \int_{\tau_*}^{\tau} \sqrt{\cos(\tau)}\,\mathrm{d}\tau \,, \quad \cos(\tau) > 0 \,.$$

The value of τ_* corresponds to the value of τ at which a motion enters the b.l. The values of x and $\dot{x}$ are obtained from

$$x = \delta\hat{x} \quad \dot{x} = \varepsilon\,\delta\,\hat{x}_\tau \,. \tag{39}$$

The separatrix crossing model then consists of two parts:

(i) away from the origin equations (35) and (36) are used, and

(ii) near the origin, equations (38) and (39) are used.

The improved model combines the averaged equations (16), (17) with this separatrix crossing model. Although it would be desirable to asymptotically *match* the two b.l. approximations with the averaged equations, this is not possible due to the unavailability of a closed form solution to the averaged equations. Instead, we numerically *patched* the averaged equations to the separatrix crossing model, as follows. As an orbit is numerically computed, the computer checks which equations are currently valid, converts to the proper variables and uses the proper model equations.

We can understand the improved model in terms of Figure 5. An orbit starting at $\tau = 0$ travels along the averaged orbit $\rho(\tau)$ until it reaches a neighborhood of the separatrix. Depending on the

orbit's phase φ at entry, the orbit may cross through the separatrix boundary layer quickly or slowly. Upon exit, the orbit begins to travel along (possibly) a different averaged $\rho(\tau)$ curve until the boundary layer is encountered again. Thus the separatrix crossing approximations determine how long a motion stays in the neighborhood of the instantaneous separatrix, and which new averaged curve $\rho(\tau)$ a motion lies on after leaving the separatrix neighborhood. In other words, the separatrix crossing model approximately determines the changes in the adiabatic invariant J (cf. Cary *et al.* [4], Henrard [14]).

Comparison of the Improved Model with the Original System

We generated a Poincaré map using the improved model for $\varepsilon = 0.1$, see Figure 9. Figure 9 exhibits many of the same features as Figure 8, but is not in complete agreement. Comparison of Figures 8 and 9 shows that Figure 9 displays an apparent discontinuity in the thread structure which may be spotted by following the threads from the origin outward around the instantaneous homoclinic loop, up to a point close to the origin, where the threads abruptly end. We have traced this flaw in Figure 9 to the numerical process which accomplishes the patching in the improved model. The discontinuity is a reflection of the necessity of prescribing to the computer a definite width of the boundary layer region of equations (35) and (36), causing a motion to remain in the boundary layer for too long a time. Presumably this deficiency of the improved model would be absent if matching (rather than patching) were possible.

In any case, the improved model offers better qualitative agreement with equation (1) than is achieved by the simplified model. This shows that the separatrix crossing model is vital to understanding the complicated dynamics of the system.

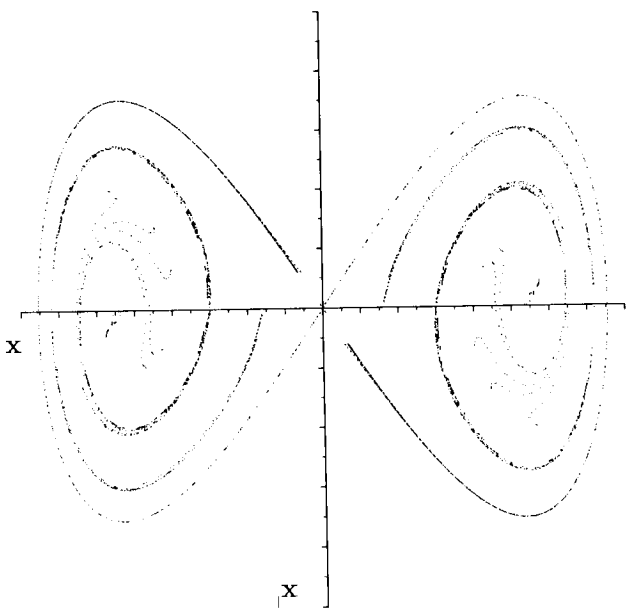

Fig. 9. The Poincaré map, computed using the improved model, for the same initial conditions (L and R) as shown in Figure 4. The improved model offers better qualitative agreement with equation (1) than is achieved by the simplified model, cf. Figure 8.

Summary

By averaging equation (1) using elliptic functions together with the simplifying assumption of instantaneous crossings of the instantaneous separatrix, we were able to reduce the Poincaré map to an interval exchange map and hence to obtain a simplified explanation (Figure 4) of the kind of chaos which is numerically observed in equation (1) and similar systems (Figure 3). However, the simplified model failed to reproduce the full complexity of the original system, cf. Figures 6, 8. By supplementing the averaging model with a separatrix crossing model, we were able to obtain better agreement with the original system, cf. Figures 8, 9.

Acknowledgement

The authors wish to thank Professor Philip Holmes of Cornell University for suggesting example (1). A preliminary version of this work was presented at the 1990 ASME International Computers in Engineering Conference [8].

Appendix I: The Unperturbed Solution

In this appendix we give the details of the treatment of the unperturbed equation by elliptic functions. We rely extensively on Byrd and Friedman [3] for calculations involving elliptic functions.

We consider equation (1) with τ fixed. For $\cos\tau < 0$, all orbits are closed and encircle the center at the origin. The period of each orbit depends on its energy h, such that as h increases from zero at the origin, the period decreases from some finite value. The solutions for x and $\dot{x}$ are written as:

$$x = r\,\mathrm{cn}(u, k)\,, \quad \dot{x} = r\,a\,\mathrm{cn}'(u, k) \tag{A1}$$

$$u = a\,t + b \tag{A2}$$

$$a^2 = r^2 - \cos\tau,\ k^2 = \frac{r^2}{2a^2} = \frac{r^2}{2(r^2 - \cos\tau)} \tag{A3}$$

$$h = \tfrac{1}{4}\,r^2(r^2 - 2\cos\tau) \tag{A4}$$

$$a > 0\,, \quad \tfrac{1}{2} \geq k^2 \geq 0\,, \quad \infty \geq r \geq 0 \tag{A5}$$

$$\mathrm{cn}' \equiv \frac{\partial\,\mathrm{cn}}{\partial u} = -\mathrm{sn}(u, k)\,\mathrm{dn}(u, k) \tag{A6}$$

where the amplitude r depends on h and b is an arbitrary constant. The cn, sn and dn functions are Jacobi elliptic functions that depend on both the argument u and modulus k. Note that both u and k depend on the amplitude r.

For $\cos\tau = 0$, all orbits are closed and encircle the degenerate center at the origin. Again, the period of each orbit depends on h, so that as h increases from zero at the origin the period

decreases from infinity. The solutions for x and $\dot{x}$ are written as in equations (A1)–(A6) with $\cos\tau = 0$. This leads to $a = r$ and $k^2 = 1/2$.

For $\cos\tau > 0$, there are three regions of closed orbits separated by a double homoclinic loop. The saddle for the loops is located at the origin. Each loop encloses a center located on either side of $(0, 0)$ at $(\pm\sqrt{\cos\tau}, 0)$. Around each center is a family of closed orbits that connect each center with its homoclinic loop. A third family of closed orbits encircles both loops. The double homoclinic loop acts as a separatrix between families of closed orbits. The solutions for x and $\dot{x}$ are found by regions, depending on the value of h in each region.

For $0 > h \geq -\frac{1}{4}\cos^2\tau$, orbits lie within the separatrix. As h decreases from zero on the separatrix, the period of the orbits decreases from infinity. The solutions for x and $\dot{x}$ are given by:

$$x = \mu\, r\, \mathrm{dn}(v, k_1)\,, \quad \dot{x} = \mu\, r\, \frac{a}{k_1}\, \mathrm{dn}'(v, k_1) \tag{A7}$$

$$v = \frac{a}{k_1}\, t + b \tag{A8}$$

$$a^2 = r^2 - \cos\tau\,, \quad k_1^2 = 2\,\frac{a^2}{r^2} = \frac{2}{r^2}\,(r^2 - \cos\tau) \tag{A9}$$

$$h = \tfrac{1}{4}\, r^2(r^2 - 2\cos\tau) \tag{A10}$$

$$a > 0\,, \quad 1 > k_1 \geq 0\,, \quad 2\sqrt{\cos\tau} > r \geq \sqrt{\cos\tau}\,, \quad \mu = \pm 1 \tag{A11}$$

$$\mathrm{dn}' \equiv \frac{\partial\, \mathrm{dn}}{\partial v} = -k_1^2\, \mathrm{sn}(v, k_1)\, \mathrm{cn}(v, k_1) \tag{A12}$$

where the amplitude r depends on h, b is an arbitrary constant, and μ is chosen depending on which loop the orbit is within: $+1$ for the right or -1 for the left.

From equation (A10), on $h = 0$, r can have 2 values, either $r = 0$ (the saddle at the origin) or $r^2 = 2\cos\tau$ (the separatrix). Points on the separatrix are considered to have infinite period since they are both forward and backward asymptotic to the saddle. The solutions for x and $\dot{x}$ are given by:

$$x = \mu\, r\, \mathrm{sech}\, u\,, \quad \dot{x} = \mu\, r\, a\, \mathrm{sech}'\, u \tag{A13}$$

$$u = a\, t + b \tag{A14}$$

$$a^2 = r^2 - \cos\tau = \cos\tau\,, \quad k^2 = 1 \tag{A15}$$

$$a > 0\,, \quad r > 0\,, \quad \mu = \pm 1 \tag{A16}$$

$$\mathrm{sech}'\, u = -\mathrm{sech}\, u \tanh u \tag{A17}$$

where b is an arbitrary constant, and μ is chosen depending on the loop: $+1$ for the right or -1 for the left.

For $h > 0$, orbits lie outside the separatrix. As h increases from zero on the separatrix, the period of the orbits decreases from infinity. The solutions for x and $\dot{x}$ are given by:

$$x = r\,\mathrm{cn}(u, k)\,, \quad \dot{x} = r\,a\,\mathrm{cn}'(u, k) \tag{A18}$$

$$u = a\,t + b \tag{A19}$$

$$a^2 = r^2 - \cos\tau\,, \quad k^2 = \frac{r^2}{2a^2} = \frac{r^2}{2(r^2 - \cos\tau)} \tag{A20}$$

$$h = \tfrac{1}{4}r^2(r^2 - 2\cos\tau) \tag{A21}$$

$$a > 0\,, \quad 1 > k \geq \tfrac{1}{2}\,, \quad \infty \geq r > 2\sqrt{\cos\tau} \tag{A22}$$

where the amplitude r depends on h and b is an arbitrary constant.

We have now found the unperturbed solutions for x and $\dot{x}$ for any value of τ. The solutions, however, do not have the same forms in all regions for all τ. This can be remedied as follows. Note that the modulus k for an elliptic function can be interpreted as a continuous parameterization of a function of the argument u. For example, the $\mathrm{cn}(u, k)$ function on $k \in [0, 1]$ can be thought of as a family of functions of u depending on k that are even, periodic, and lie between $+1$ and -1. The value of k specifies a particular member of the family by defining the period of the function. In fact, $\mathrm{cn}(u, 0) = \cos(u)$ and $\mathrm{cn}(u, 1) = \mathrm{sech}(u)$, so that the cn function connects cosine with sech as k goes from 0 to 1. This allows us to use cn instead of sech on the separatrix.

For those orbits which lie inside the separatrix, the solution is naturally written interms of the dn function, cf. equation (A7). However, we can use cn instead of dn as follows: We extend the domain of definition of $\mathrm{cn}(u, k)$ from the usual range $k \in [0, 1]$ to $k \in [0, \infty]$ by employing a classical transformation which replaces k by $1/k$ as the modulus in the cn function [3]:

$$\textit{Transformation Rules for } k_1 = \frac{1}{k} \tag{A23}$$

$$\mathrm{cn}(u, k) = \mathrm{dn}(v, k_1)\,, \quad \mathrm{dn}(u, k) = \mathrm{cn}(v, k_1)\,, \quad \mathrm{sn}(u, k) = k_1\,\mathrm{sn}(v, \mathrm{k}_1)$$

$$u = k_1 v\,, \quad K = k_1 K_1\,, \quad E(u) = \frac{1}{k_1}\,[E(v) - k_1'^2 v]\,, \quad E = \frac{1}{k_1}\,(E_1 - k_1'^2 K_1)$$

$$v = ku\,, \quad K_1 = kK\,, \quad E(v) = \frac{1}{k}[E(u) - k'^2 u]\,, \quad E_1 = \frac{1}{k}\,[E - k'^2 K]$$

$$K \equiv K(k)\,, \quad K_1 \equiv K(k_1)\,, \quad E \equiv E(k)\,, \quad E_1 \equiv E(k_1)$$

$$E(u) \equiv E(am(u, k), k)\,, \quad E(v) = E(am(v, k_1), k_1)$$

$$k'^2 = 1 - k^2\,, \quad k_1'^2 = 1 - k_1^2\,.$$

In (A23), $\{u, E(u), K, E\}$ are variables that use k while $\{v, E(v), K_1, E_1\}$ use k_1. Both u and v are incomplete elliptic integrals of the first kind with their completions denoted K and K_1, respectively. Both $E(u)$ and $E(v)$ are incomplete elliptic integrals of the second kind with the completions denoted E and E_1, respectively. Using (A23), we can extend the domain of definition of $\mathrm{cn}(u, k)$ to include values for $k > 1$. Thus the cn function for $k > 1$ is the same as the dn function for $k_1 = 1/k < 1$.

This completes the derivation of equations (7) and (8) in the text.

Appendix II: Variation of Parameters

In this appendix we give the details of the application of the method of variation of parameters to equation (1).

Let r and u in equation (7) be functions of t. Then differentiating x in equation (7), we find

$$\frac{\mathrm{d}x}{\mathrm{d}t} = \mu\, \dot{r}\, \mathrm{cn} + \mu\, r \left(\mathrm{cn}'\, \dot{u} + \frac{\partial\, \mathrm{cn}}{\partial k}\, \dot{k} \right) \tag{B1}$$

where

$$\dot{k} = -\frac{k^3}{r^3} \left[2\, \dot{r} \cos \tau + \varepsilon r \sin \tau \right] . \tag{B2}$$

Differentiating $\dot{x}$ in equation (7), we find

$$\frac{\mathrm{d}\dot{x}}{\mathrm{d}t} = \mu\, \mathrm{cn}' \left[r\, \dot{a} + a\, \dot{r} \right] + \mu\, r\, a \left[\mathrm{cn}''\, \dot{u} + \frac{\partial\, \mathrm{cn}'}{\partial k}\, \dot{k} \right] \tag{B3}$$

where

$$\dot{a} = \frac{r}{a}\, \dot{r} + \varepsilon\, \frac{\sin \tau}{2a} . \tag{B4}$$

We now require the expressions for $\dot{x}$ in equations (B1) and (7) to be equal, and we substitute equation (B3) for $\ddot{x}$ into equation (1) in order to obtain a system of two equations in the two unknowns $\dot{r}$ and $\dot{u}$. Then we solve for $\dot{r}$ and $\dot{u}$ and simplify using the following relations [3]:

$$\mathrm{cn}'' = (2k^2 - 1 - 2k^2\, \mathrm{cn}^2)\, \mathrm{cn} \tag{B5}$$

$$\mathrm{cn}'^2 = 1 - k^2 + (2k^2 - 1)\, \mathrm{cn}^2 - k^2\, \mathrm{cn}^4 \tag{B6}$$

$$\mathrm{cn}'\, \frac{\partial\, \mathrm{cn}'}{\partial k} = \frac{1}{2}\, \frac{\partial}{\partial k}\, (\mathrm{cn}'^2) = -k(1 - \mathrm{cn}^2)^2 + \mathrm{cn}''\, \frac{\partial\, \mathrm{cn}}{\partial k} \tag{B7}$$

$$\frac{\partial\, \mathrm{cn}}{\partial k} = -\mathrm{cn}'\, \frac{\mathrm{d}u}{\mathrm{d}k} . \tag{B8}$$

Note that u depends on k so that $\partial\, \mathrm{cn}'/\partial k = \partial/\partial k\ (\partial\, \mathrm{cn}/\partial u) \neq \partial/\partial u\ (\partial\, \mathrm{cn}/\partial k)$ and that $\mathrm{d}u/\mathrm{d}k$ is well-defined:

$$k\, k'^2\, \frac{\mathrm{d}u}{\mathrm{d}k} = E(u) - k'^2 u + \frac{1}{\mathrm{dn}}\, \mathrm{dn}' . \tag{B9}$$

This is found by applying Leibnitz's rule to u, where u depends on both the independent variables θ and k:

$$u = F(\theta, k) = \int_0^{\theta} \{1 - k^2 \sin(\rho)\}^{-1/2}\, \mathrm{d}\rho . \tag{B10}$$

We used the computer algebra system MACSYMA to perform all these computations [19, 20], which resulted in equations (10) and (11) in the text.

References

1. Arnold, V. I., *Mathematical Methods of Classical Mechanics*, Springer, New York, 1984.
2. Bender, C. M. and Orzag, S. A., *Advanced Mathematical Methods for Scientists and Engineers*, McGraw-Hill, New York, 1978.
3. Byrd, P. and Friedman, M., *Handbook of Elliptic Integrals for Engineers and Physicists*, Springer, Berlin, 1954.
4. Cary, J. R., Escande, D. F., and Tennyson, J. L., 'Adiabatic-invariant change due to separatrix crossing', *Phys. Rev. A* **34**, 1986, 4256–4275.
5. Cary, J. R. and Skodje, R. T., 'Phase change between separatrix crossings', *Physica D* **36**, 1989, 287–316.
6. Coppola, V. T., *Averaging of Strongly Nonlinear Oscillators Using Elliptic Functions*, Ph.D. Dissertation, Cornell University, 1989.
7. Coppola, V. T. and Rand, R. H., 'Averaging using elliptic functions: Approximation of limit cycles', *Acta Mechanica* **81**, 1990, 125–142.
8. Coppola, V. T. and Rand, R. H., 'Computer algebra, elliptic functions and chaos', in *Proceedings of 1990 ASME International Computers in Engineering Conference*, Vol. 1, Boston, Aug. 6–10, 1990, 193–200.
9. Devaney, R., *An Introduction to Chaotic Dynamics*, Addison-Wesley, New York, 1987.
10. Escande, D. F., 'Hamiltonian Chaos and Adiabaticity', preprint.
11. Goldstein, H., *Classical Mechanics*, 2nd ed., Addison-Wesley, Reading, Mass, 1980.
12. Greenwood, D., *Principles of Dynamics*, Prentice Hall, Englewood Cliffs, N.J., 1965.
13. Guckenheimer, J. and Holmes, P., *Nonlinear Oscillations, Dynamical Systems, and Bifurcations of Vector Fields*, Springer, New York, 1983.
14. Henrard, J., 'The adiabatic invariant in classical mechanics', preprint.
15. Kath, W. K., 'Slowly varying phase plane and boundary-layer theory', *Studies in Applied Math.* **72**, 1985, 221–239.
16. Keane, M., 'Interval exchange transformations', *Math. Z.* **141**, 1975, 25–31.
17. Kevorkian, J. and Cole, J. D., *Perturbation Methods in Applied Mathematics*, Springer, New York, 1981.
18. Menyuk, C. R., 'Particle motion in the field of a modulated wave', *Phys. Rev. A* **31**, 1985, 3282–3290.
19. Rand, R. H., *Computer Algebra in Applied Mathematics: An Introduction to MACSYMA*, Pitman, Boston, 1984.
20. Rand, R. H. and Armbruster, D., *Perturbation Methods, Bifurcation Theory and Computer Algebra*, Springer, New York, 1987.
21. Sanders, J. A. and Verhulst, F., *Averaging Methods in Nonlinear Dynamical Systems*, Springer, New York, 1985.
22. Shaw, S. W. and Wiggins, S., 'Chaotic dynamics of a whirling pendulum', *Physica D* **31**, 1988, 190–211.
23. Simmonds, J. and Mann, J., *A First Look at Perturbation Theory*, Kreiger Publishing, Malabar, FL, 1986.
24. Timofeev, A. V., 'On the constancy of an adiabatic invariant when the nature of the motion changes', *Sov. Phys. JETP* **48**, 1978, 656–659.
25. Wiggins, S., 'On the detection and dynamical consequences of orbits homoclinic to hyperbolic periodic orbits and normally hyperbolic invariant tori in a class of ordinary differential equations', *SIAM J. Appl. Math.* **48**, 1988, 262–285.